A Consistent Rate Constant for the Reaction of Nitrogen Dioxide with Oxygen Atom

Yan Li[a], Sandra Javoy[b], Remy Mevel[c], and Xuefei Xu[a]

[a] Center for Combustion Energy, Department of Energy and Power Engineering, and Key Laboratory for Thermal Science and Power Engineering of Ministry of Education, Tsinghua University, Beijing 100084, China

[b] University of Orléans, Department of Chemistry, 1, Rue de Chartres, BP 6759, 45067 Orléans Cedex 02, France.

[c] Center for Combustion Energy, School of Vehicle and Mobility, and State Key Laboratory for Automotive Safety and Energy, Tsinghua University, Beijing 100084, China

This supplemental material includes summary tables of the rate constant data we employed to update the rate constant of the reaction $NO_2+O=NO+O_2$. The cartesian coordinates and absolute electronic energies of the optimized structures are then given. Finally, we are proposing a large selection of modeling results for various hydrogen-NO_x mixtures.

1 Rate constant data

Table 1: The calculated rate constants k for the reaction of $NO_2+O=NO+O_2$ in the temperature range of 1000-3000 K.

T (K)	k ($cm^3mol^{-1}s^{-1}$)
200	6.56E+12
298.15	2.77E+12
300	2.74E+12
400	1.94E+12
500	1.69E+12
600	1.62E+12
800	1.70E+12
1000	1.93E+12
1060	2.01E+12
1200	2.22E+12
1400	2.57E+12
1600	2.95E+12
1780	3.32E+12
1800	3.37E+12
2000	3.81E+12
2300	4.52E+12
2500	5.01E+12
2700	5.53E+12
3000	6.32E+12

Table 2: The rate constants from the experimental data by Estupian et al. (2001EST/NIC9697-9703) [1].

T (K)	k ($cm^3mol^{-1}s^{-1}$)
221	8.74E+12
230	8.33E+12
240	7.93E+12
294	6.43E+12
296	6.39E+12
298	6.35E+12
300	6.31E+12
339	5.69E+12
350	5.54E+12
357	5.46E+12
360	5.42E+12
387	5.14E+12
412	4.93E+12

413	4.92E+12
420	4.87E+12
425	4.83E+12

2 Molecules geometry and electronic energy

Cartesian coordinates and absolute electronic energies of optimized structures by TPSSh/MG3S.

NO_2: -205.15783408 a.u.

Atomic type	Coordinates (Å)		
	X	Y	Z
N	0.00000000	0.00000000	0.32226700
O	0.00000000	1.10224000	-0.14099200
O	0.00000000	-1.10224000	-0.14099200

O: -75.09350623 a.u.

Atomic type	Coordinates (Å)		
	X	Y	Z
O	0.00000000	0.00000000	0.00000000

TS (^{2}A"): -280.2537811 a.u.

Atomic type	Coordinates (Å)		
	X	Y	Z
N	-0.91641900	0.04937100	0.00000000
O	-0.89045000	-1.13187600	0.00000000
O	1.69231700	0.22113400	0.00000000
O	0.00000000	0.86754200	0.00000000

NO: -129.93885904 a.u.

Atomic type	Coordinates (Å)		
	X	Y	Z
N	0.00000000	0.00000000	-0.61327300
O	0.00000000	0.00000000	0.53661400

O$_2$: -150.37872792 a.u.

Atomic type	Coordinates (Å)		
	X	Y	Z
O	0.00000000	0.00000000	0.60415000
O	0.00000000	0.00000000	-0.60415000

3 Additional modeling results

3.1 Nitrogen dioxide pyrolysis
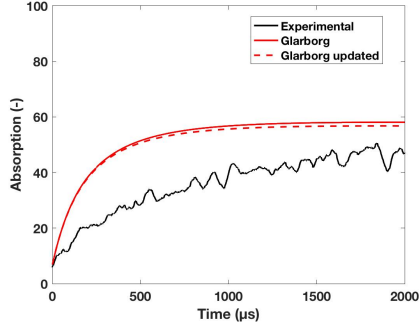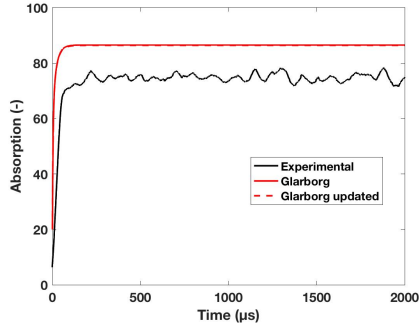

X$_{N2O}$=40.1 ppmv; T=1492 K; P=339 kPa   X$_{N2O}$=40.1 ppmv; T=1511 K; P=330 kPa
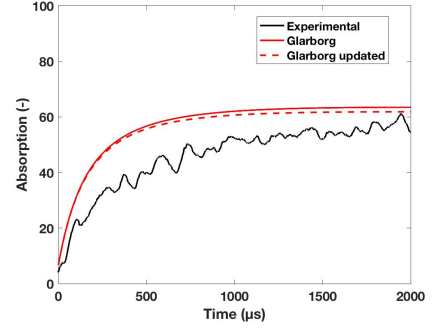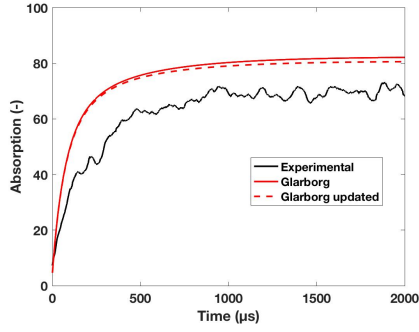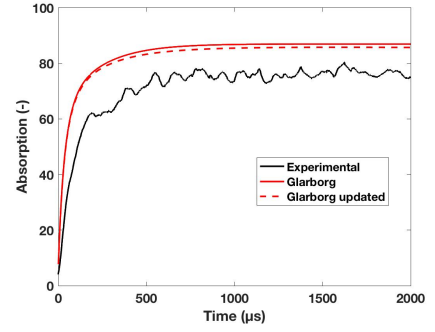
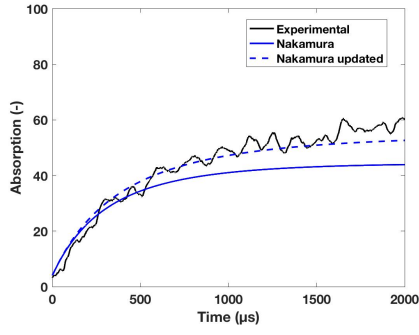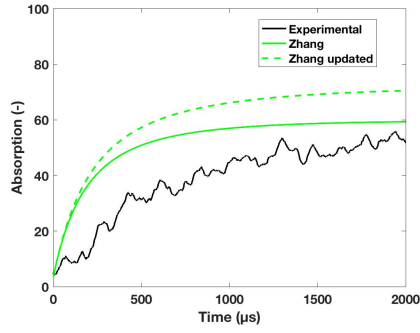X$_{N2O}$=20 ppmv; T=1648 K; P=313 kPa   X$_{N2O}$=40.1 ppmv; T=1650 K; P=325 kPa

X$_{N2O}$=20 ppmv; T=2019 K; P=288 kPa   X$_{N2O}$=15 ppmv; T=2053 K; P=270 kPa
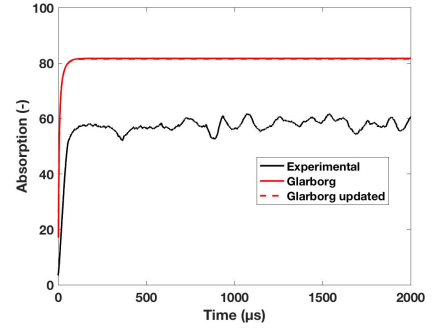
Figure 1: Experimental and predicted total absorption at 130.5 nm during NO$_2$ pyrolysis. Model of Glarborg et al. [2].

X$_{N2O}$=20 ppmv; T=1564 K; P=324 kPa   X$_{N2O}$=40.1 ppmv; T=1585 K; P=325 kPa
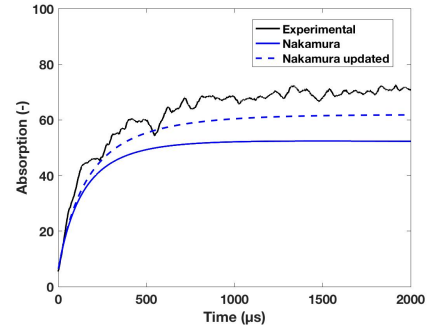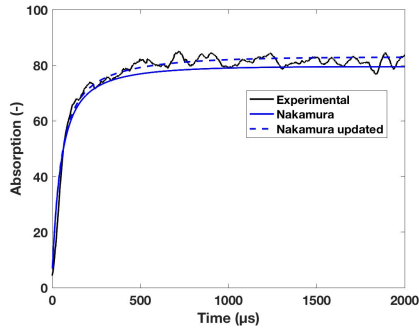
X$_{N2O}$=40.1 ppmv; T=1719 K; P=306 kPa   X$_{N2O}$=20 ppmv; T=1769 K; P=298 kPa
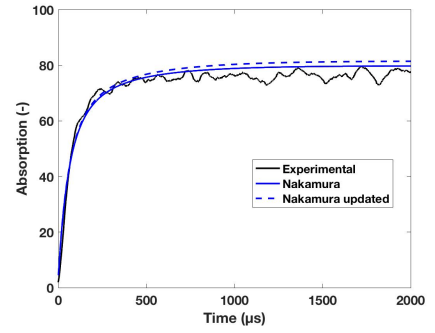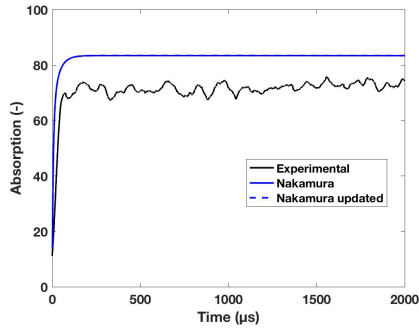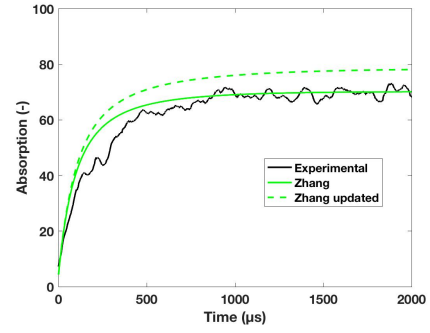
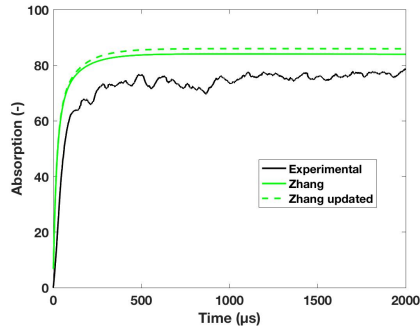X$_{N2O}$=18 ppmv; T=2117 K; P=268 kPa   X$_{N2O}$=18 ppmv; T=2187 K; P=274 kPa
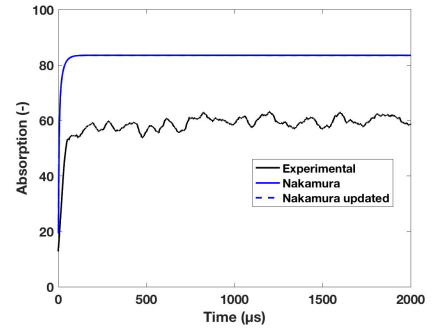
Figure 2: Experimental and predicted total absorption at 130.5 nm during NO$_2$ pyrolysis. Model of Nakamura et al. [3].
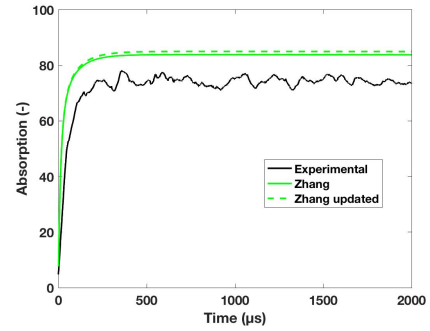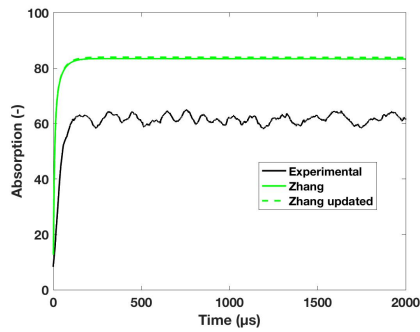
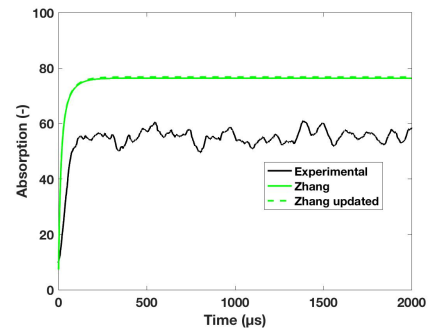X_{N2O}=15 ppmv; T=1598 K; P=326 kPa X_{N2O}=20 ppmv; T=1648 K; P=313 kPa

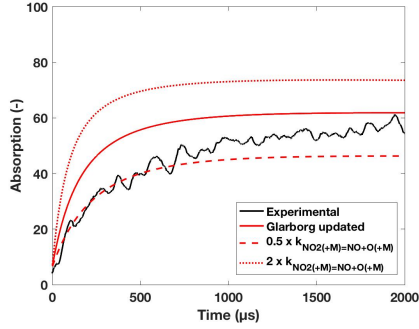X_{N2O}=20 ppmv; T=1830 K; P=302 kPa X_{N2O}=18 ppmv; T=1896 K; P=290 kPa

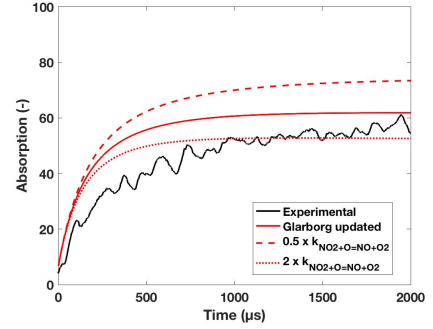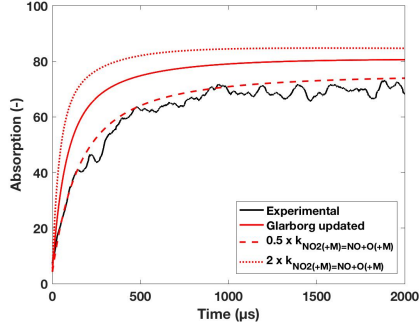X_{N2O}=5 ppmv; T=1877 K; P=886 kPa X_{N2O}=5 ppmv; T=1896 K; P=563 kPa

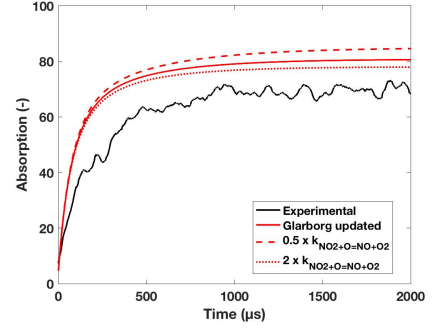Figure 3: Experimental and predicted total absorption at 130.5 nm during NO_2 pyrolysis. Model of Zhang et al. [4].
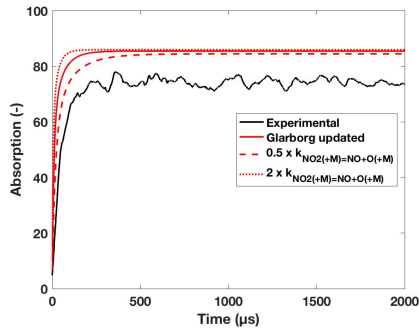
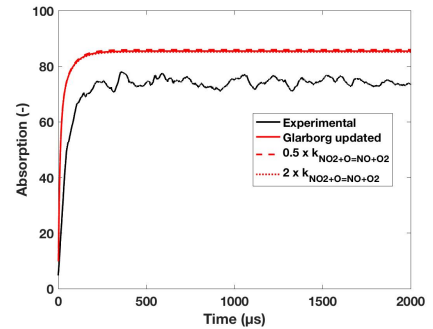X$_{N2O}$=40.1 ppmv; T=1511 K; P=330 kPa   X$_{N2O}$=40.1 ppmv; T=1511 K; P=330 kPa

X$_{N2O}$=20 ppmv; T=1648 K; P=313 kPa   X$_{N2O}$=20 ppmv; T=1648 K; P=313 kPa

X$_{N2O}$=18 ppmv; T=1896 K; P=290 kPa   X$_{N2O}$=18 ppmv; T=1896 K; P=290 kPa

Figure 4: Effect of k_1 and k_2 on the total absorption during NO_2-Ar mixtures pyrolysis at different temperature. k_1 corresponds to the rate constant of $NO_2(+M)=NO+O(+M)$. k_2 corresponds to the rate constant of $NO_2+O=NO+O_2$. Left column: k_1 was perturbed. Right column: k_2 was perturbed. The updated model of Glarborg et al. [2] has been used.
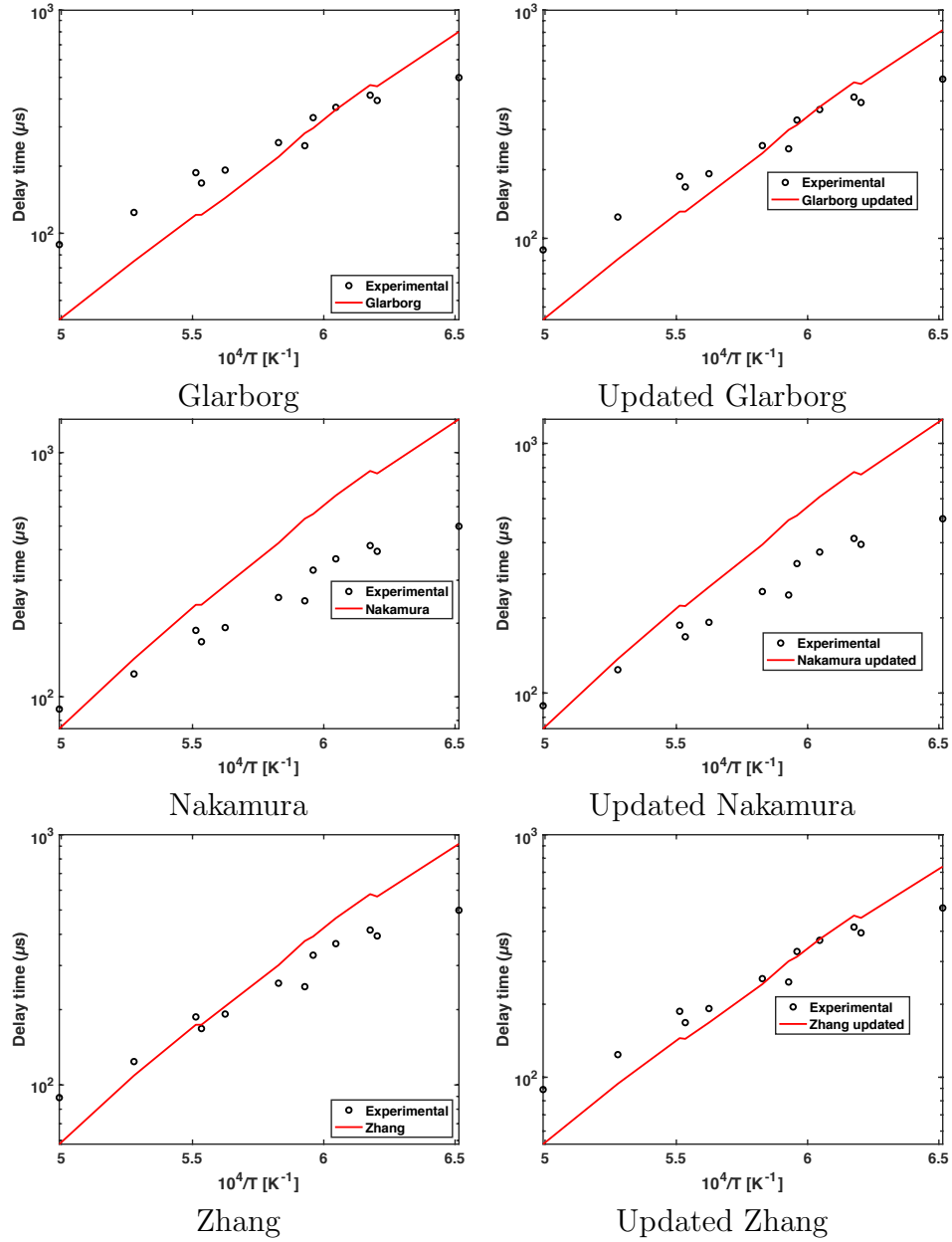
3.2 Hydrogen oxidation by nitrogen dioxide

Figure 5: Experimental[5] and predicted delay-time during the oxidation of H_2 by NO_2. The delay-time is defined as the time needed for the OH^* signal to decrease to 50% of the peak value. Mixture: X_{H2}=0.00222, X_{NO2}=0.00392, X_{Ar}=0.99386. T=1535-2003 K; P=105-124 kPa.
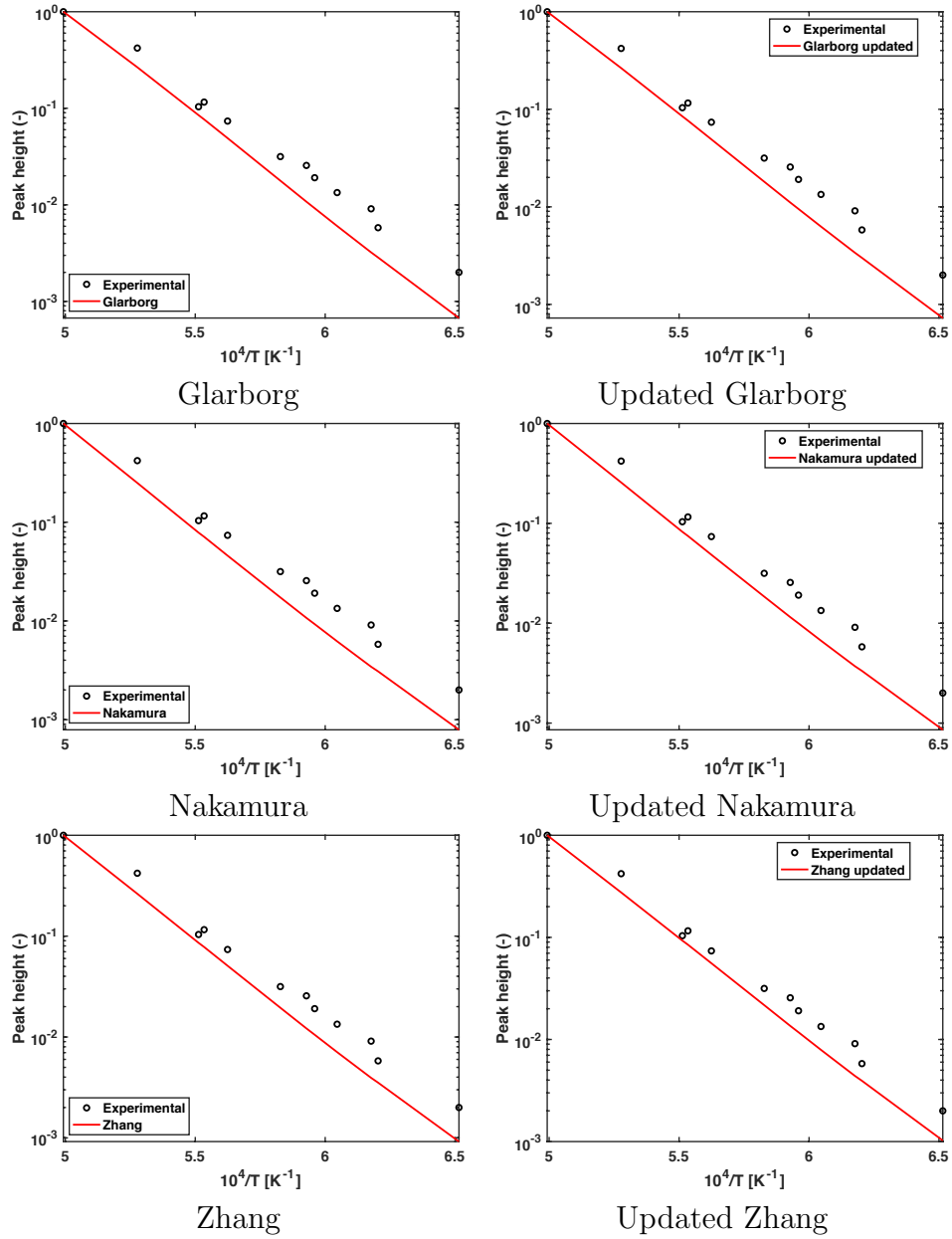
Figure 6: Experimental[5] and predicted normalized OH* peak height during the oxidation of H_2 by NO_2. Mixture: X_{H2}=0.00222, X_{NO2}=0.00392, X_{Ar}=0.99386. T=1535-2003 K; P=105-124 kPa.

Figure 7: Experimental[5] and predicted normalized OH* profiles during the oxidation of H_2 by NO_2. Mixture: X_{H2}=0.00222, X_{NO2}=0.00392, X_{Ar}=0.99386. Model of Glarborg et al. [2].

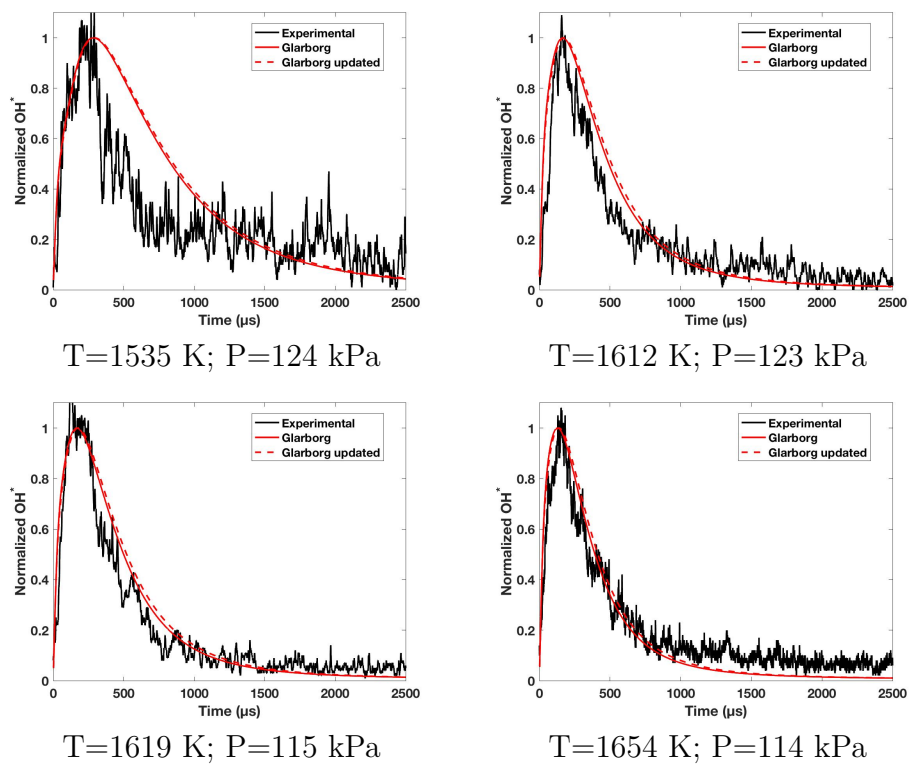Figure 8: Experimental[5] and predicted normalized OH* profiles during the oxidation of H_2 by NO_2. Mixture: X_{H2}=0.00222, X_{NO2}=0.00392, X_{Ar}=0.99386. Model of Nakamura et al. [3].
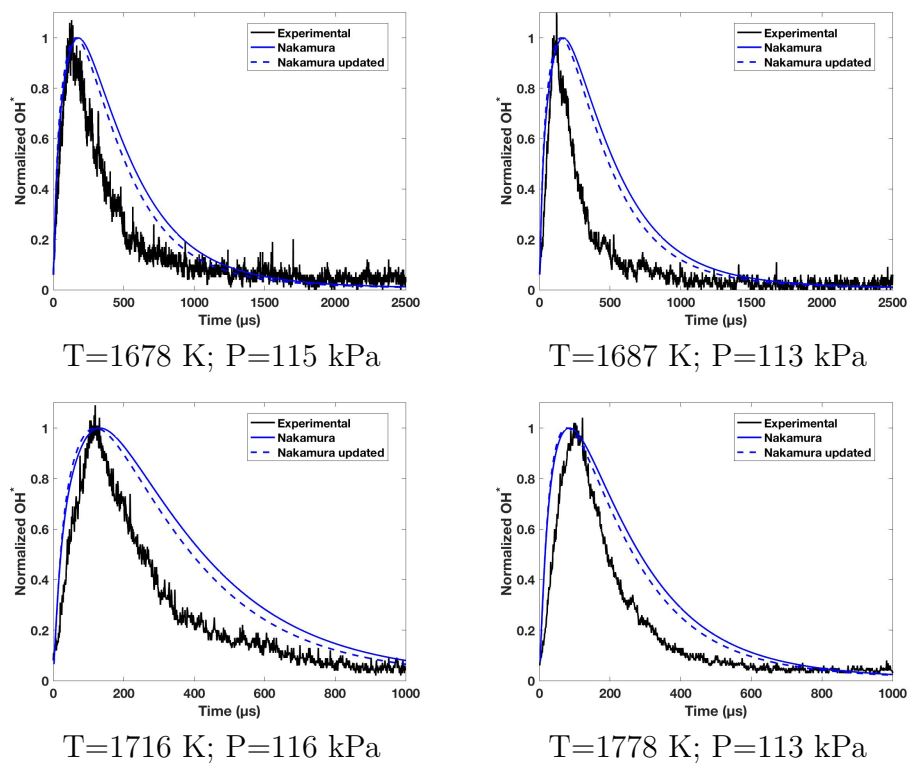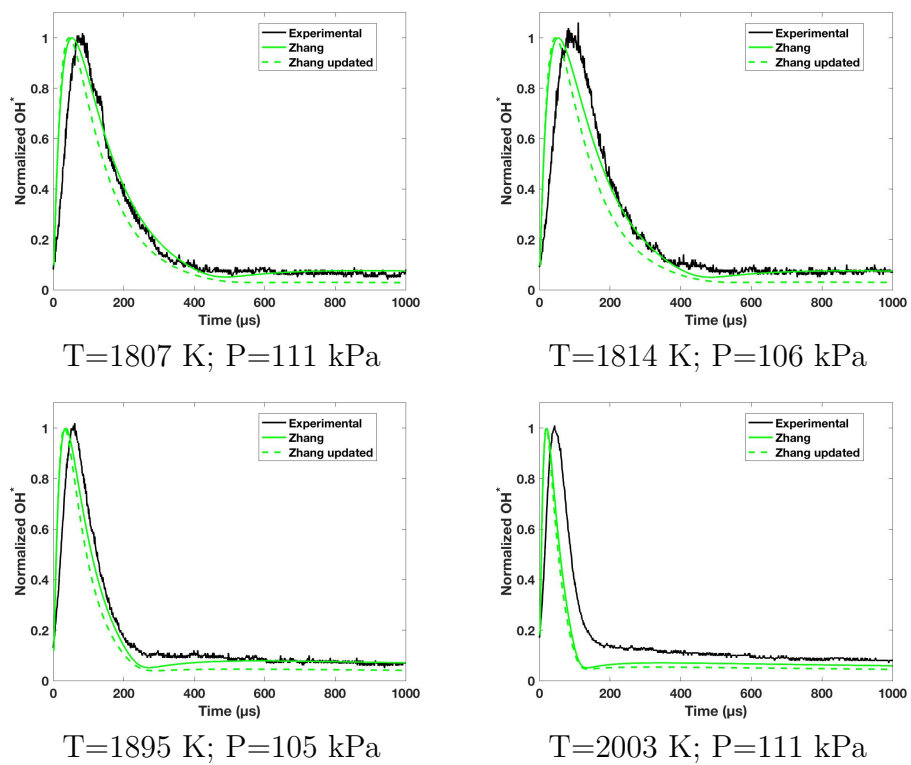
Figure 9: Experimental[5] and predicted normalized OH* profiles during the oxidation of H_2 by NO_2. Mixture: X_{H2}=0.00222, X_{NO2}=0.00392, X_{Ar}=0.99386. Model of Zhang et al. [4].

Glarborg   Updated Glarborg

Glarborg   Updated Glarborg

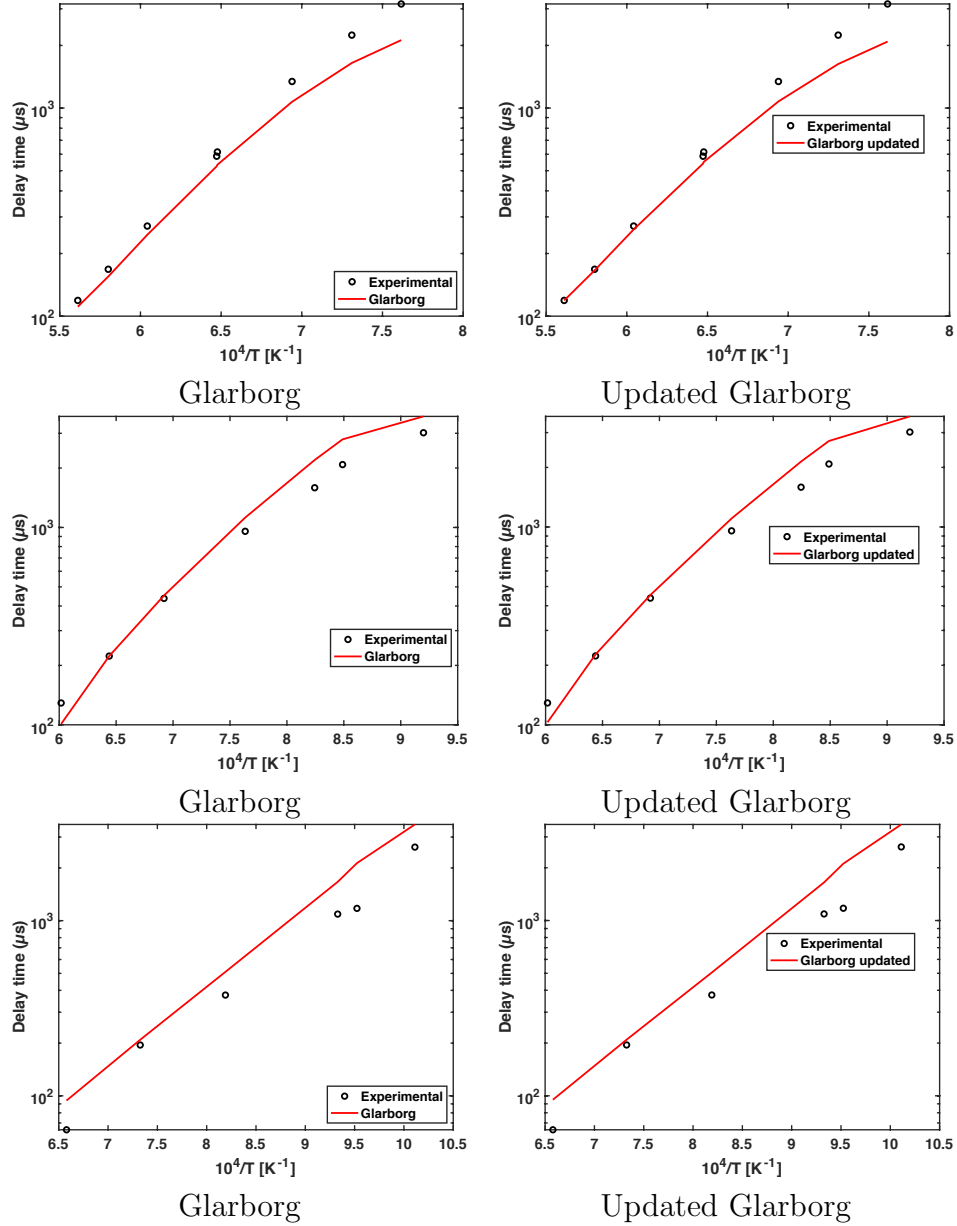Glarborg   Updated Glarborg

Figure 10: Experimental[6] and predicted delay-time during the oxidation of H_2 by NO_2. The delay-time is defined as the time needed for the H_2O concentration to reach 50% of its maximum value within the experimental test time. In top figures, Mix 1: $X_{H2}=0.00222$, $X_{NO2}=0.00375$, $X_{Ar}=0.99403$. In middle figures, Mix 2: $X_{H2}=0.00444$, $X_{NO2}=0.00178$, $X_{Ar}=0.99378$. In bottom figures, Mix 3: $X_{H2}=0.01778$, $X_{NO2}=0.00168$, $X_{Ar}=0.98054$. T=989-1782 K, P=97-128 kPa. Results obtained with the model of Glarborg et al. [2] and its updated version.
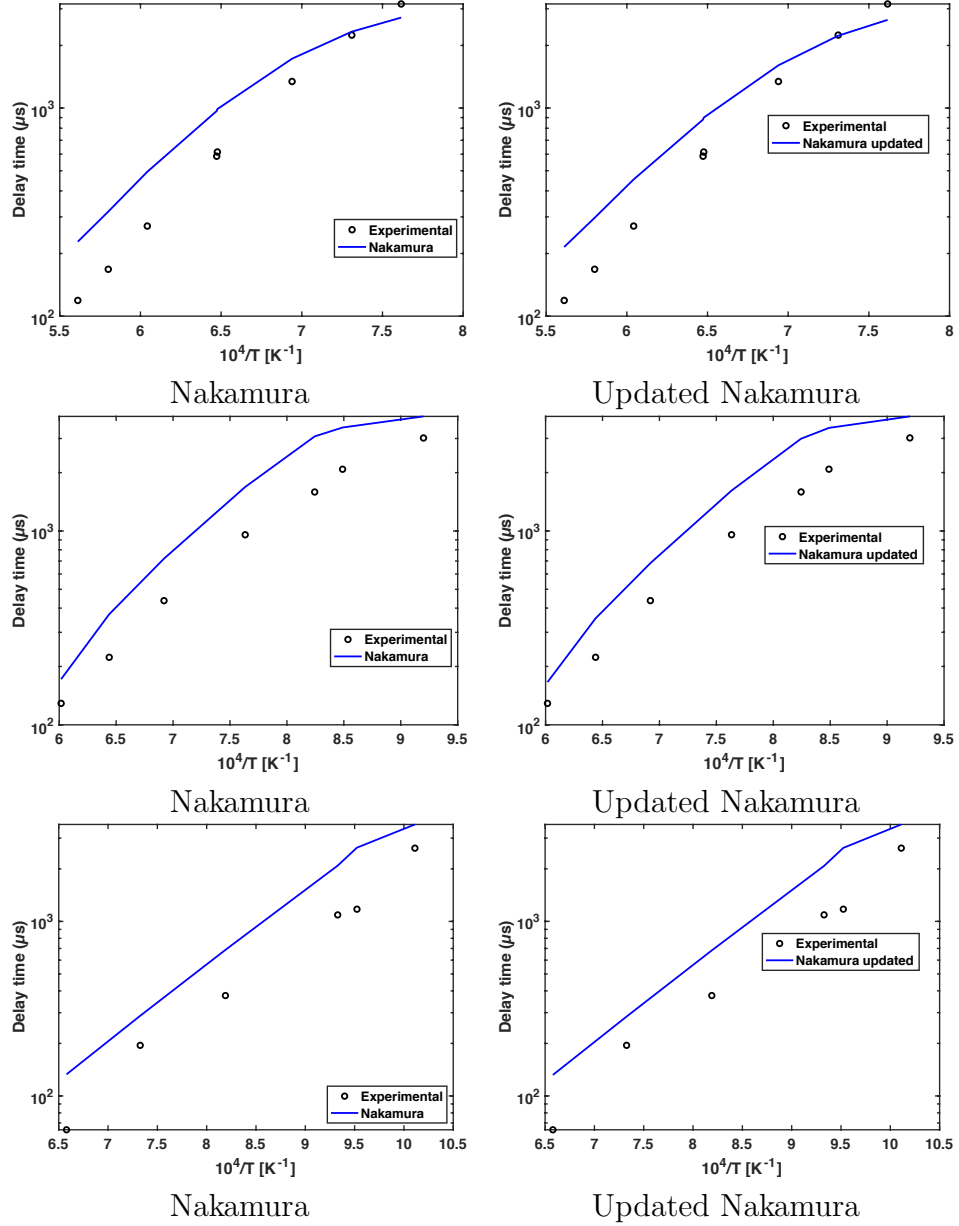
Figure 11: Experimental[6] and predicted delay-time during the oxidation of H_2 by NO_2. The delay-time is defined as the time needed for the H_2O concentration to reach 50% of its maximum value within the experimental test time. In top figures, Mix 1: X_{H2}=0.00222, X_{NO2}=0.00375, X_{Ar}=0.99403. In middle figures, Mix 2: X_{H2}=0.00444, X_{NO2}=0.00178, X_{Ar}=0.99378. In bottom figures, Mix 3: X_{H2}=0.01778, X_{NO2}=0.00168, X_{Ar}=0.98054. T=989-1782 K, P=97-128 kPa. Results obtained with the model of Nakamura et al. [3] and its updated version.
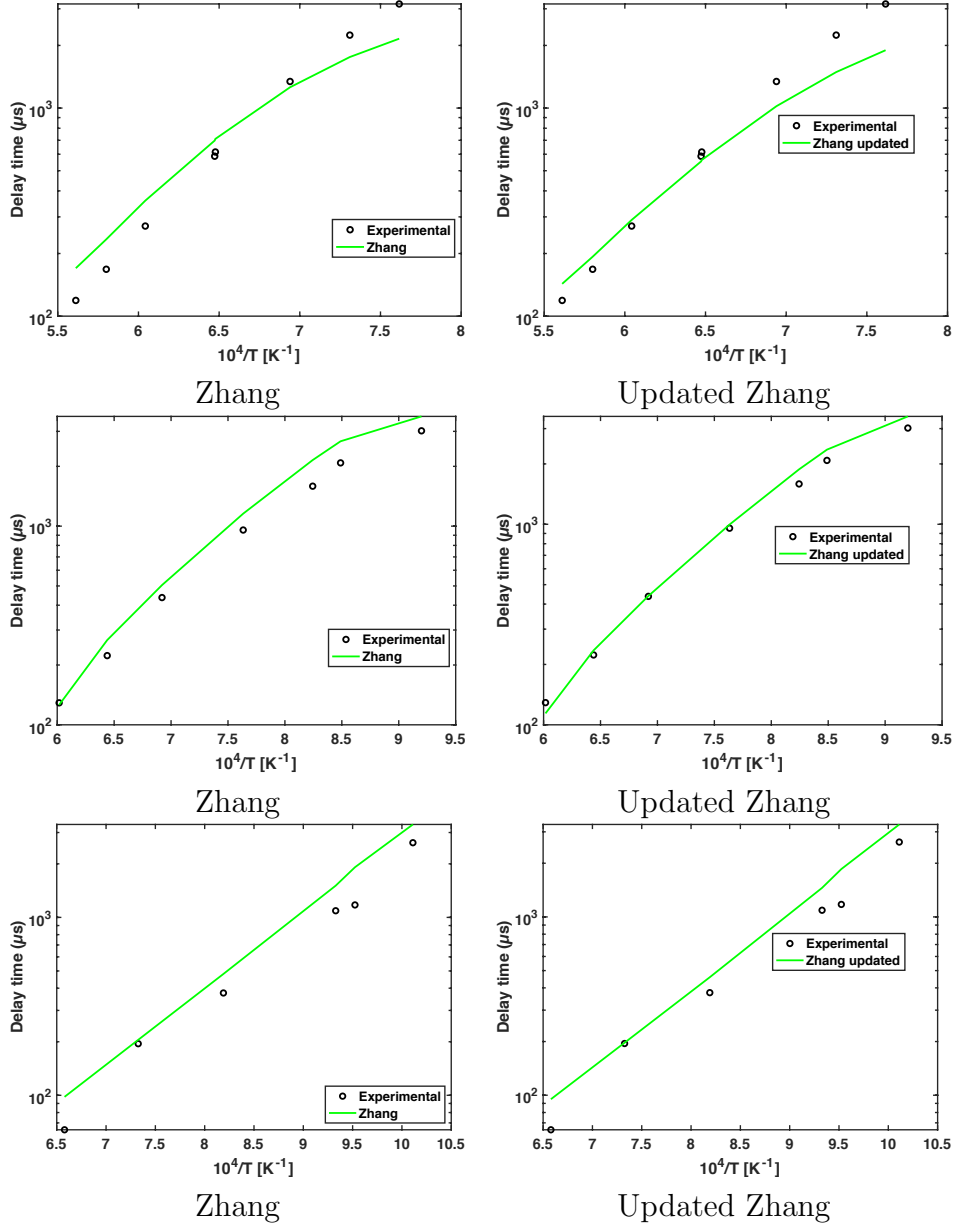
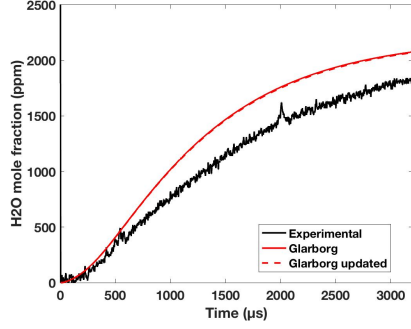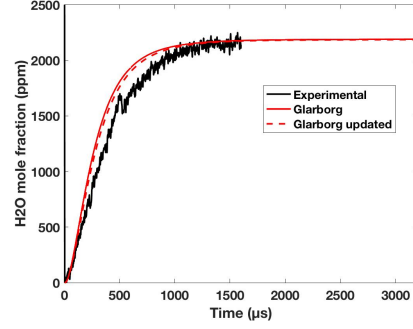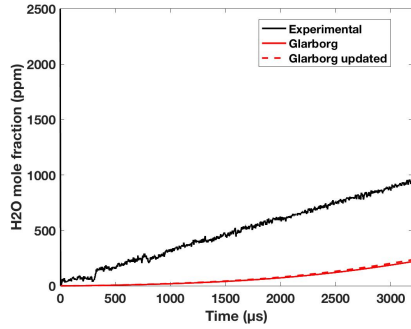Figure 12: Experimental[6] and predicted delay-time during the oxidation of H_2 by NO_2. The delay-time is defined as the time needed for the H_2O concentration to reach 50% of its maximum value within the experimental test time. In top figures, Mix 1: X_{H2}=0.00222, X_{NO2}=0.00375, X_{Ar}=0.99403. In middle figures, Mix 2: X_{H2}=0.00444, X_{NO2}=0.00178, X_{Ar}=0.99378. In bottom figures, Mix 3: X_{H2}=0.01778, X_{NO2}=0.00168, X_{Ar}=0.98054. T=989-1782 K, P=97-128 kPa. Results obtained with the model of Zhang et al. [4] and its updated version.

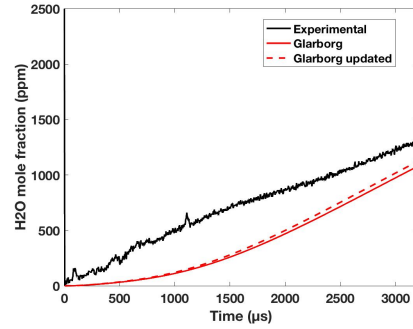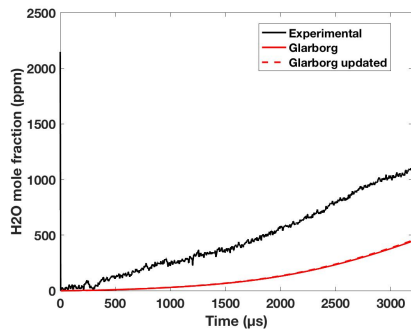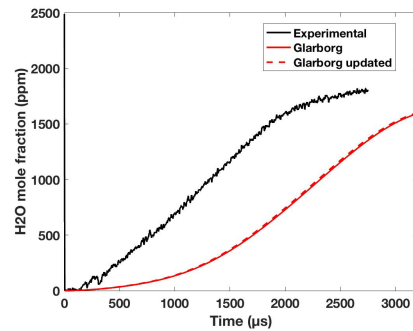Figure 13: Experimental[6] and predicted H_2O profiles during the oxidation of H_2 by NO_2. Mix 1: X_{H2}=0.00222, X_{NO2}=0.00375, X_{Ar}=0.99403; Mix 2: X_{H2}=0.00444, X_{NO2}=0.00178, X_{Ar}=0.99378. Mix 3: X_{H2}=0.01778, X_{NO2}=0.00168, X_{Ar}=0.98054. Model of Glarborg et al. [2].
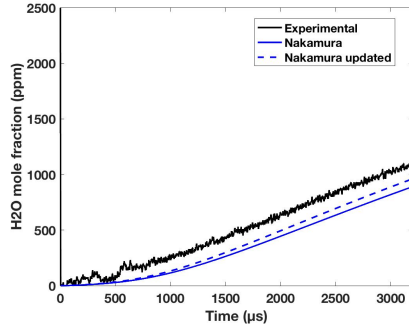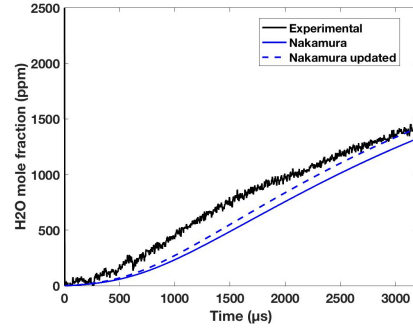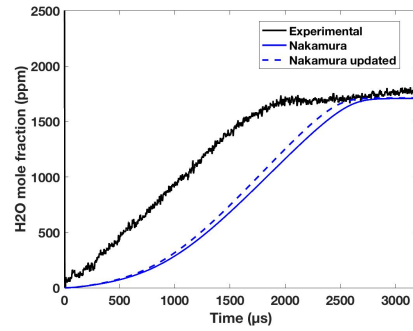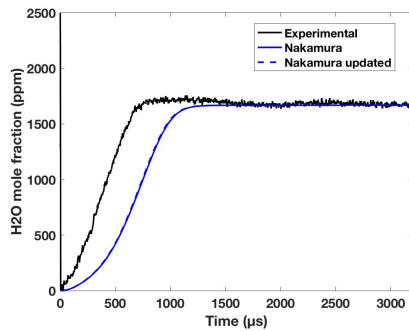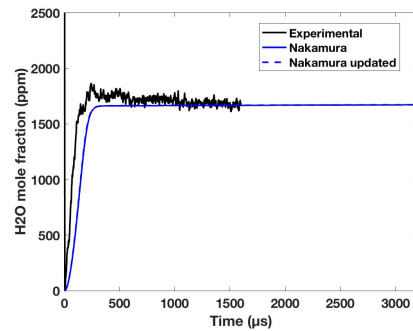
Figure 14: Experimental[6] and predicted H_2O profiles during the oxidation of H_2 by NO_2. Mix 1: X_{H2}=0.00222, X_{NO2}=0.00375, X_{Ar}=0.99403; Mix 2: X_{H2}=0.00444, X_{NO2}=0.00178, X_{Ar}=0.99378. Mix 3: X_{H2}=0.01778, X_{NO2}=0.00168, X_{Ar}=0.98054. Model of Nakamura et al. [3].
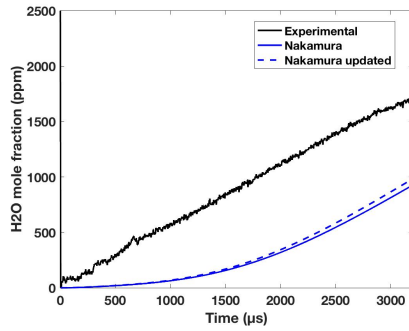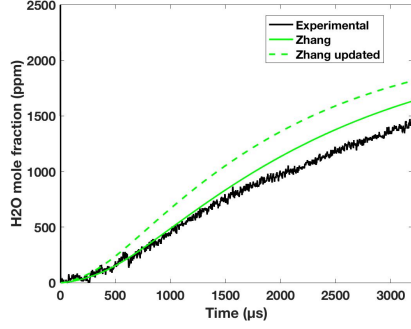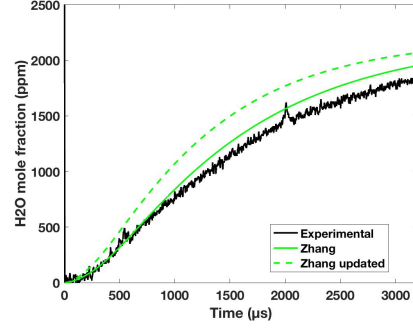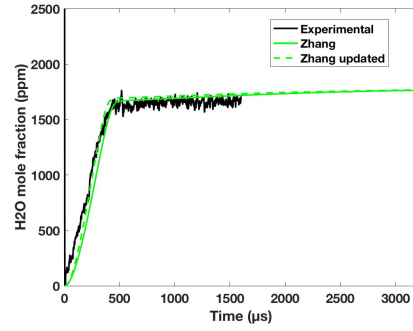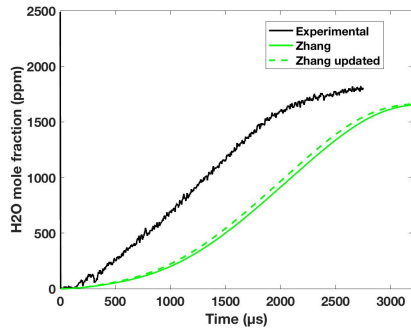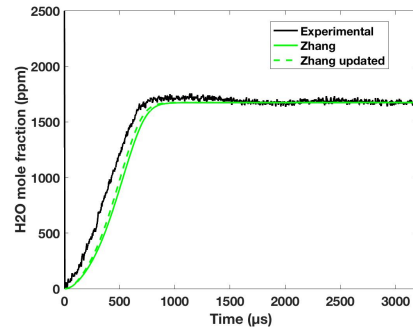
Figure 15: Experimental[6] and predicted H_2O profiles during the oxidation of H_2 by NO_2. Mix 1: X_{H2}=0.00222, X_{NO2}=0.00375, X_{Ar}=0.99403; Mix 2: X_{H2}=0.00444, X_{NO2}=0.00178, X_{Ar}=0.99378. Mix 3: X_{H2}=0.01778, X_{NO2}=0.00168, X_{Ar}=0.98054. Model of Zhang et al. [4].

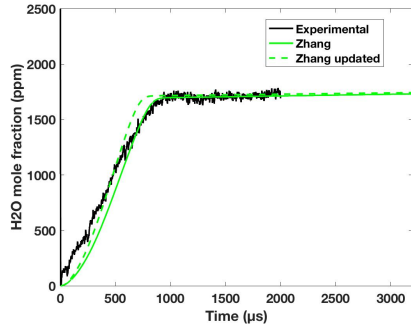## 3.3 Hydrogen oxidation by nitrogen dioxide and oxygen
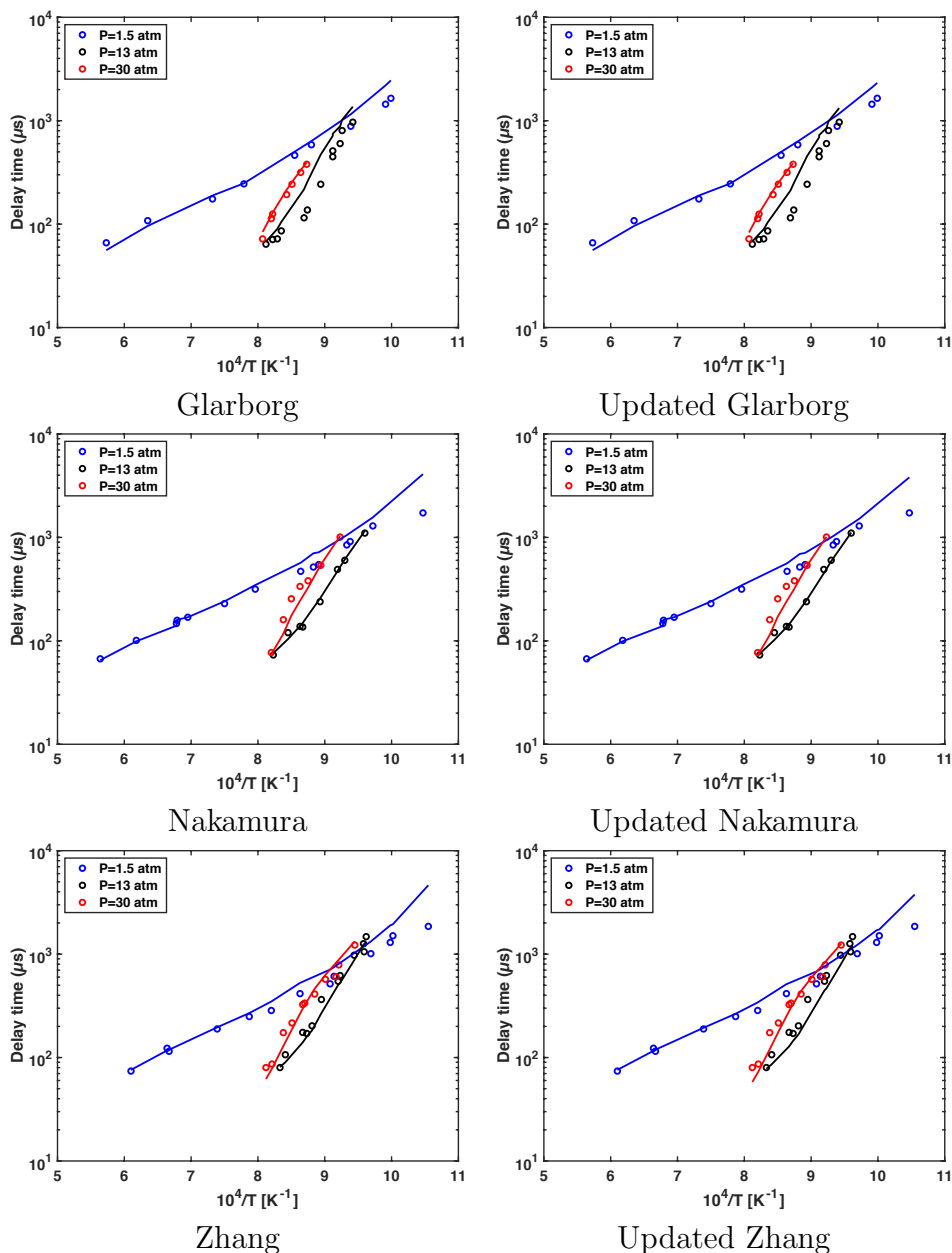
Figure 16: Experimental[7] and predicted delay-time during the oxidation of H_2 by O_2 with NO_2 addition. The delay-time is defined as the base-line extrapolated maximum slope of the OH^* signal. In top figures: $\Phi=0.3$, $X_{NO2}=100$ ppm, $X_{Ar}=0.9799$. In middle figures: $\Phi=1$, $X_{NO2}=100$ ppm, $X_{Ar}=0.9799$. In bottom figures: $\Phi=0.5$, $X_{NO2}=100$ ppm, $X_{Ar}=0.9799$. Results obtained with the models of Glarborg et al. [2], of Nakamura et al. [3], and of Zhang et al. [4] and its updated version.

3.4 Hydrogen oxidation by nitrogen oxides and dioxygen

a): Φ=0.1, X_{NO2}=70 ppm, X_{N2}=0.93993, τ=0.24 s, P=101 kPa.

b): Φ=1, X_{NO2}=70 ppm, X_{N2}=0.98493, τ=0.24 s, P=101 kPa.

c): Φ=0.1, X_{NO}=250 ppm, X_{N2}=0.93975, τ=0.24 s, P=101 kPa

d): Φ=0.2, X_{NO}=240 ppm, X_{N2}=0.96476, τ=0.24 s, P=101 kPa

e): Φ=0.1, X_{NO}=220 ppm, X_{N2}=0.93978, τ=1 s, P=1 MPa.

f): Φ=0.2, X_{NO}=220 ppm, X_{N2}=0.96478, τ=1 s, P=1 MPa.

Figure 17: Experimental[8] and predicted species profiles during the oxidation in a jet-stirred reactor of H_2 by O_2 with NO addition. In top figures: Glarborg et al. [2] and its updated version. In middle figures: Nakamura et al. [3] and its updated version. In bottom figures: Zhang et al. [4] and its updated version. Original models: solid lines. Updated models: dashed lines.
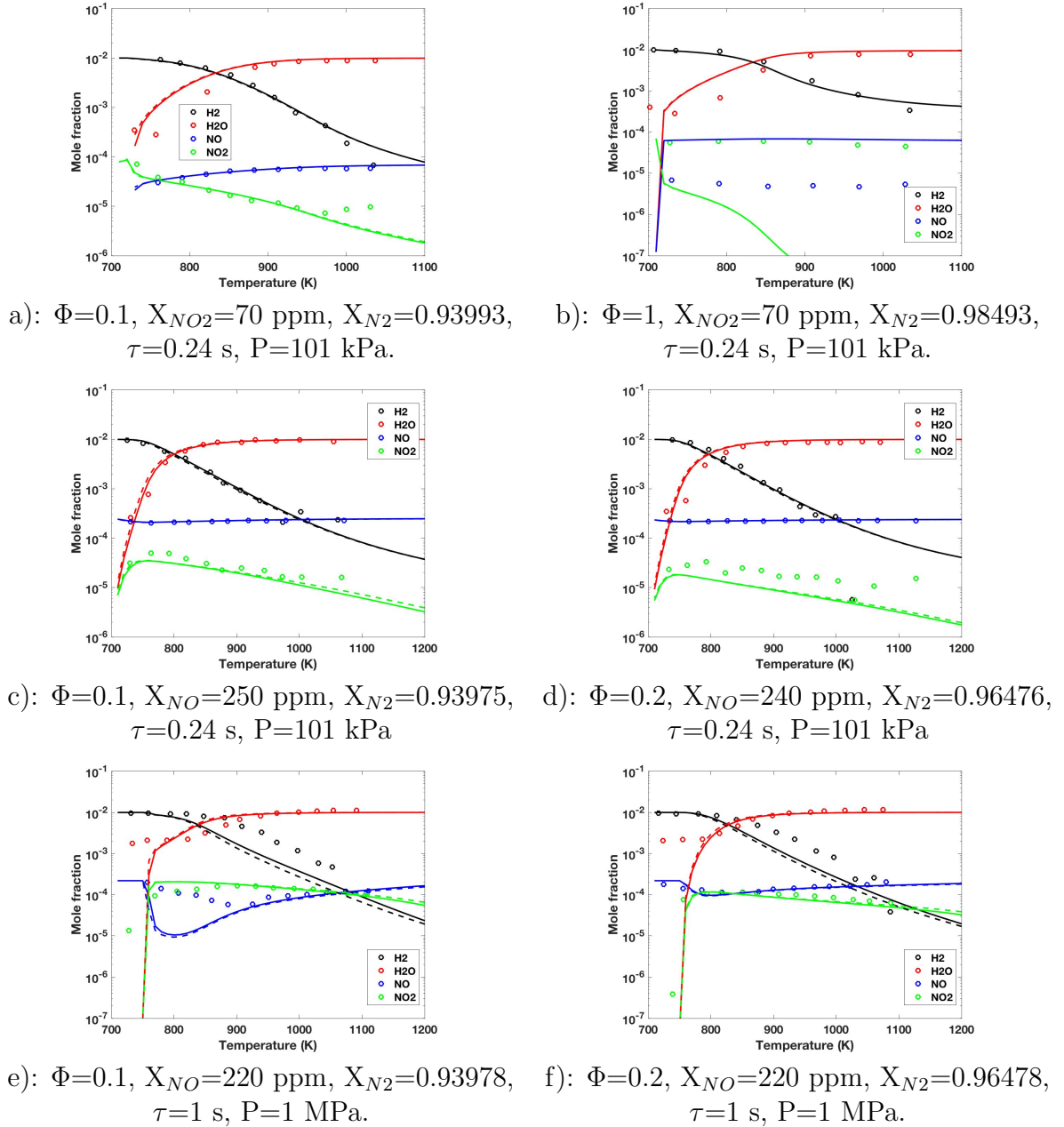
References

[1] **Estupian E., Nicovich J. and Wine P.**: A temperature-dependent kinetics study of the important stratospheric reaction $O(^{3P})+NO_2 \rightarrow O_2+NO$. *The Journal of Physical Chemistry A*, 2001, vol 105, n° 42, p. 9697–9703.

[2] **Glarborg P., Miller J., Ruscic B. and Klippenstein S.**: Modeling nitrogen chemistry in combustion. *Progress in Energy and Combustion Science*, 2018, vol 67, p. 31–68.

[3] **Nakamura H., Hasegawa S. and Tezuka T.**: Kinetic modeling of ammonia/air weak flames in a micro flow reactor with a controlled temperature profile. *Combustion and Flame*, 2017, vol 185, p. 16–27.

[4] **Zhang Y., Mathieu O., Petersen E., Bourque G. and Curran H.**: Assessing the predictions of a NOx kinetic mechanism on recent hydrogen and syngas experimental data. *Combustion and Flame*, 2017, vol 182, p. 122 – 141.

[5] **Mulvihill C. and Petersen E.**: OH^* chemiluminescence in the H_2-NO_2 and H_2-N_2O systems. *Combustion and Flame*, 2020, vol 213, p. 291–301.

[6] **Mulvihill C., Mathieu O. and Petersen E.**: H_2O time histories in the H_2-NO_2 system for validation of NOx hydrocarbon kinetics mechanisms. *International Journal of Chemical kinetics*, 2019, vol 51, n° 9, p. 669–678.

[7] **Mathieu O., Levacque A. and Petersen E.**: Effects of NO2 addition on hydrogen ignition behind reflected shock waves. *Proceedings of the Combustion Institute*, 2013, vol 34, p. 633–640.

[8] **Dagaut P. and Dayma G.**: Effects of air contamination on the combustion of hydrogen - Effect of NO and NO_2 addition on hydrogen ignition and oxidation kinetics. *Combustion Science and Technology*, 2006, vol 178, p. 1999–2024.